

## Determination of Mossbauer Electric Field Gradient

V. K. GARG

*Departamento de Física e Química, Universidade Federal do Espírito Santo,  
29000 Vitória, ES, Brasil*

Recebido em 12 de Maio de 1980

There are several reports of the electric quadrupole interactions available in the literature.<sup>1-4</sup> The present discussion is a short survey, introducing the electric quadrupole up to the experimental polarised studies.

Existem várias publicações sobre interações de quadrupolo elétrico na literatura - "A presente discussão é um resumo, introduzindo o quadrupolo elétrico até o nível de recentes estudos experimentais.

### 1. INTRODUCTION, (t STANDARD FORM OF EFG

The magnitude of the quadrupole splitting is pronortional to the Z componerit of the electric field gradient (EFG) tensor which interacts with the quadrupole moment of the nucleus. For  $I = 3/2$ , the quadrupole splitting can be expressed as

$$Q.S. = \frac{1}{2} e^2 q Q (1 + \eta^2/3)^{1/2} \quad (1)$$

Where  $Q$  is the quadrupole moment of the nucleus

$$e q = V_{zz} = - \text{the Z component of the EFG} \quad (2)$$

$e$  = proton charge

and  $\eta$  is the asymmetry parameter

$$\frac{V_{xx} - V_{yy}}{V_{zz}}$$

Either  $q$  or  $V_{zz}$  is referred to as the field gradient. The EFG tensor has nine components.

The potential at the Mössbauer nucleus (located at the origin) due to point charge  $q$  at  $(x, y, z)$  a distance  $r = (x^2 + y^2 + z^2)^{1/2}$  from the origin is given by

$$V = q/r \quad (3)$$

The negative gradient of this potential,  $-\vec{\nabla}V$ , is the electric field,  $\vec{E}$ , at the nucleus, with components

$$E_x = -\frac{\delta V}{\delta x} = qx r^{-3}, \quad E_y = -\frac{\delta V}{\delta y} = qy r^{-3}, \quad E_z = -\frac{\delta V}{\delta z} = qz r^{-3} \quad (4)$$

the gradient of the electric field at the nucleus,  $\vec{\nabla}\vec{E}$ , is given by

$$\vec{\nabla}\vec{E} = -\vec{\nabla}\vec{\nabla}V = (\text{EFG}) = - \begin{vmatrix} V_{xx} & V_{xy} & V_{xz} \\ V_{yx} & V_{yy} & V_{yz} \\ V_{zx} & V_{zy} & V_{zz} \end{vmatrix}, \quad \begin{aligned} V_{xx} &= \frac{\delta^2 V}{\delta x^2}, & V_{xy} &= \frac{\delta^2 V}{\delta x \delta y} \\ V_{xz} &= \frac{\delta^2 V}{\delta x \delta z}, & \text{etc} \end{aligned} \quad (5)$$

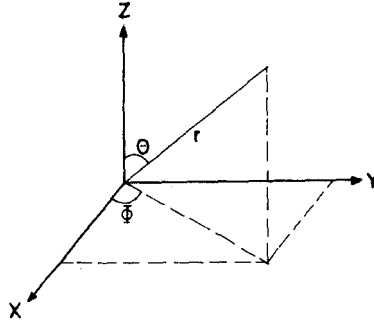
the second partial derivative tensor components are

$$\begin{aligned} V_{xx} &= q(3x^2 - r^2)r^{-5}, \\ V_{yy} &= q(3y^2 - r^2)r^{-5}, \\ V_{zz} &= q(3z^2 - r^2)r^{-5}, \\ V_{xy} &= V_{yx} = 3qxy r^{-5}, \\ V_{xz} &= V_{zx} = 3qxz r^{-5}, \\ V_{yz} &= V_{zy} = 3qyz r^{-5}. \end{aligned} \quad (6)$$

The EFG components can be expressed in spherical coordinates as

$$\begin{aligned} r &= (x^2 + y^2 + z^2)^{1/2}, \quad \theta = \cos^{-1}(z/r), \quad \phi = \tan^{-1}(y/x), \\ x &= r \sin\theta \cos\phi, \quad y = r \sin\theta \sin\phi, \quad z = r \cos\theta \end{aligned}$$

$$\begin{aligned}
 V_{xx} &= q(3 \sin^2 \theta \cos^2 \phi - 1)r^{-3} \\
 V_{yy} &= q(3 \sin^2 \theta \sin^2 \phi - 1)r^{-3} \\
 V_{zz} &= q(3 \cos^2 \theta - 1)r^{-3} \\
 V_{xy} = V_{yx} &= 3qr^{-3} \sin^2 \theta \sin \phi \cos \phi \\
 V_{xz} = V_{zx} &= 3qr^{-3} \sin \theta \cos \theta \cos \phi \\
 V_{yz} = V_{zy} &= 3qr^{-3} \sin \theta \cos \theta \sin \phi
 \end{aligned} \tag{7}$$



The total contribution to each EFG components is obtained by simply adding the individual contributions. If the coordinate axes are properly chosen, the above tensor can be reduced to diagonal form so that the EFG can be completely specified by the three components  $V_{xx}$ ,  $V_{yy}$  and  $V_{zz}$ . These components are also not independent and are related by Laplace's equation

$$V_{xx} + V_{yy} + V_{zz} = 0 \tag{8}$$

reducing the number of independent parameter to two,  $V_{zz}$  and  $\eta$  where

$$\eta = \frac{V_{xx} - V_{yy}}{V_{zz}} \tag{9}$$

The value of EFG tensor components obviously depend upon the choice of the coordinate axes. For this reason a standard form of EFG tensor is expressed by defining a unique set of axes known as the principal axes of the EFG tensor. This unique coordinate system is the one for which the off-diagonal components are zero and diagonal components are ordered, such that

$$|V_{zz}| \geq |V_{yy}| \geq |V_{xx}| \tag{10}$$

this restricts  $0 \leq \eta \leq 1$ . Now, only two of the five independent parameters of the EFG tensor seem to be left. Actually, however, three independent off-diagonal elements have been replaced by the Euler angles  $(\alpha, \beta, \gamma)$  necessary to describe the relative orientation of the principal and initial axes. The orientation parameters affect the line intensities in single crystal spectra.

Many properties of the EFG tensor can be deduced from the symmetry properties of the molecule or crystal. Often the Z axis of the EFG coincides with the highest symmetry axis of the molecule or crystal. The Z axis of EFG, and the X and Y axes, do not always coincide with metal - ligand bond directions. In such cases, it is necessary to choose an arbitrary set of axes, work out the EFG components, diagonalise the tensor, and then choose  $|V_{zz}| \geq |V_{yy}| \geq |V_{xx}|$ .

If the electronic configuration has a symmetry lower than cubic, electrons about the Mössbauer atom also contribute to the EFG tensor.

## 2. CORE POLARISATION

The field gradient which is finally produced at the Mössbauer nucleus, say iron, is modified by the presence of the inner closed-shell electrons. While these core electrons themselves do not contribute to the field gradient, they are polarised by the field gradient of the lattice and valence electrons. This effect is accounted for by the Sternheimer<sup>5</sup> antishielding parameters. The total field gradient at the nucleus is expressed<sup>6</sup> as

$$\frac{V_{zz}}{e} = q = (1 - R)q_{\text{valence}} + (1 - \gamma_{\infty})q_{\text{lattice}} \quad (11)$$

$$\frac{V_{xx} - V_{yy}}{e} = \eta q = (1 - R)_{\text{ion}} q_{\text{ion}} + (1 - \gamma_{\infty})q_{\text{lattice}}$$

The subscript 'ion' and 'lattice' stand for the charge distribution of the spherical  $3d$  valence electrons belonging to the fer-

rous ( $5D\ 3d^6$ ) and the neighbouring ion in the crystalline lattice respectively.  $(1-R)$  and  $(1-\gamma_\infty)$  are the Sternheimer factors which have been introduced to correct for the polarisation of the ferric like ( $6S_2\ 3d^5$ ) core by the EFG of the ion and the lattice charge distribution. For  $Fe^{2+}$   $R = 0.32^7$ ,  $\gamma_\infty = -10.6^8$  and for  $Fe^{3+}$   $\gamma_\infty = -9.1^9$ . The other distribution to the EFG tensor consists of the uncompensated  $3d$  electrons. In octahedral symmetry<sup>10</sup>, the  $3d$  electrons are split into two groups. Those transforming as  $T_{2g}$  are largely unaffected, since these do not ordinarily participate in bonding to ligands. These are usually termed as  $d_{xy}$ ,  $d_{xz}$  and  $d_{yz}$  and represent electric charge concentrated in regions other than along the ligand directions. The  $E_g$  electrons,  $d_{z^2}$  and  $d_{x^2-y^2}$ , couple with ligand orbitals produce antibonding wavefunctions. These concentrate the charge along the bond directions. As a result, these  $E_g$  electrons occupy a higher energy level than  $T_{2g}$  electrons.

The magnitude of splitting of these groups of electrons has a profound effect on the magnetic and Mössbauer properties of these compounds. Weak ligands, such as  $OH^-$ ,  $H_2O$ ,  $NH_3$  and the halogens produce relatively small splitting. The five or six  $3d$  electrons of ferric or ferrous compounds fill by Hund's rule for maximum multiplicity. Strong ligands such as  $CN$ , pyridine or  $10$ -phenanthroline cause a greater splitting and lead to the filling of  $T_{2g}$  Shell.

For an electron in a state  $\psi$  the electric field gradient has the expectation value.

$$\langle q \rangle = - \frac{\langle 3 \cos^2\theta - 1 \rangle}{\langle r^3 \rangle} \quad (12)$$

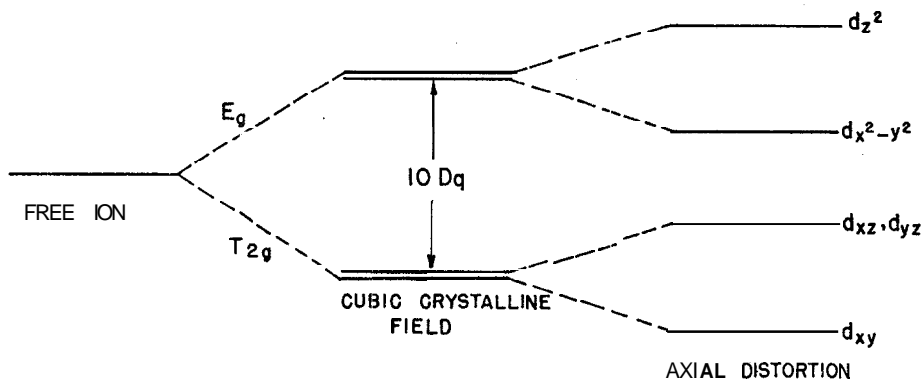
These expectation values have been calculated using  $\psi_{3d} R(r) Y_l^m(\theta, \phi)$ . The values of  $\langle 3 \cos^2\theta - 1 \rangle$  are independent of  $R(r)$  and are easily found<sup>11</sup> from various  $p$ ,  $d$  orbitals.

TABLE

Expectation values of  $q_{\text{valence}}$  for  $p$  and  $d$  electrons

Wave function	$\frac{V_{zz}}{e} = q_{\text{valence}}$	Wave function	$\frac{V_{zz}}{e} = q_{\text{valence}}$	Symmetry representation
$p_x$	$+\frac{2}{5} \langle r^{-3} \rangle_p$	$d_{z^2}$	$-\frac{4}{7} \langle r^{-3} \rangle_d$	$E_g$
$p_y$	$+\frac{2}{5} \langle r^{-3} \rangle_p$	$d_{x^2-y^2}$	$+\frac{4}{7} \langle r^{-3} \rangle_d$	
$p_z$	$-\frac{4}{5} \langle r^{-3} \rangle_p$	$d_{xy}$	$+\frac{4}{7} \langle r^{-3} \rangle_d$	
		$d_{xz}$	$-\frac{2}{7} \langle r^{-3} \rangle_d$	$T_{2g}$
		$d_{yz}$	$-\frac{2}{7} \langle r^{-3} \rangle_d$	

It is clear from symmetry considerations that as long as  $d$ -orbitals are degenerate,  $\langle q \rangle_{\text{valence}} = 0$ . Even under the influence of a cubic crystalline field, the field gradient at the nucleus will vanish since the degenerate  $T_{2g}$  and  $E_g$  states both retain spherical symmetry. Distortions from cubic symmetry, however, remove the degeneracy of the states and if the non-degenerate  $d$ -orbitals are unequally populated, a field gradient is produced.



The two situations which can produce a non zero  $\langle q \rangle_{\text{valence}}$  are spin free  $\text{Fe}^{2+}$  (six  $d$ -electrons) and spin paired  $\text{Fe}^{3+}$  (five  $d$ -electrons) in an axially distorted octahedra field (with negative ligands). At  $0^\circ\text{K}$  the electrons populate only the lowest possible states and one obtains the limiting field gradient for these two cases. Ingalls<sup>11</sup> has treated the field gradient in spin - free ferrous complexes in much more detail. He obtains a reduction factor to include the effects of finite temperature (Boltzman distribution) and of spin - orbit coupling. Now

$$q \approx (1 - R)q_{\text{valence}} = - (1-R) \langle 3\cos^2\theta - 1 \rangle \langle r^{-3} \rangle_{3d} \quad (13)$$

since  $(1-R) > 0$  and  $\langle r^{-3} \rangle_{3d} > 0$  the sign determining factor is  $\langle 3\cos^2\theta - 1 \rangle$ , which may be positive or negative depending on the manner in which the electrons are distributed among the  $d$ -orbitals.

The relative magnitude of these two effects, ligand disposition and uncompensated  $3d$  electrons change completely with ligand strength. Ligands, sufficiently weak that the  $\text{Fe}^{3+}$  high spin electron configuration is obtained, do not cause observable EFG. The uncompensated  $3d$ -electron in  $\text{Fe}^{2+}$  high spin compounds causes a large quadrupole splitting. The mixed strong - weak ligand case,  $\text{Fe}^{3+}$  (O-phenthroline)<sub>2</sub> $\text{Cl}_3^{-3}$  which has no  $3d$  electron contribution to the EFG does not yield a resolved doublet. The cyanides lie at the other extreme,  $\text{K}_3|\text{Fe}^{2+}(\text{CN})_6|$ , has a zero splitting in consequence of its balanced ligands and filled  $T_{2g}$  structure.  $\text{K}_3|\text{Fe}^{3+}(\text{CN})_6| \cdot 3\text{H}_2\text{O}$  has one  $T_{2g}$  electron missing, but yields only a small splitting (0.3 mm/sec). This illustrates the nephelauxetic effect of strong ligands, in which the ligands force the  $T_{2g}$  electrons away from the nucleus where the  $\langle r^{-3} \rangle$  is considerably smaller. The effect of ligand symmetry is correspondingly enhanced. Consider two diamagnetic ferrous compounds in which no odd  $3d$  electrons affect the EFG tensor. The very strong (greater than  $12 \text{CN}^-$ ) ligand  $\text{NO}^+$  causes a splitting of 1.70 mm/sec. in sodium nitroprusside.<sup>12</sup> In  $\text{Na}_4|\text{Fe}(\text{CN})_5\text{NO}_2| \cdot 2\text{H}_2\text{O}$  the weaker ligand ( $\text{NO}_2$ ) results in a splitting of 0.86 mm/sec.

The choice of basis for  $3d$  electrons is normally either  $dz^2$ ,  $dx^2-y^2$ ,  $d_{xy}$ ,  $dxz$ ,  $dyz$  or  $d_0$ ,  $d_{\pm 1}$ ,  $d_{\pm 2}$ . Each of the wave functions in

these alternate bases has zero asymmetry parameter. There exists, however, other  $3d$  - wavefunctions with asymmetry parameter differing from zero and even attaining the values of unity. Consider the wavefunction

$$\psi = (d_{xz} + i\lambda d_{yz}) / (1 + \lambda^2)^{1/2}$$

where  $\lambda$  is a real number, the EFG tensor is

$$\text{EFG} = -\frac{2}{7} \begin{pmatrix} 1 - 2\lambda^2 & 0 & 0 \\ 0 & -2 + \lambda^2 & 0 \\ 0 & 0 & 1 + \lambda^2 \end{pmatrix} \frac{q \langle r^{-3} \rangle}{1 + \lambda^2} \quad (14)$$

The mixing coefficient  $\lambda$  depends on the details of the distribution and the nature of metal - ligand interaction. It might be supposed that such a wave function are idle speculation. However, the EFG tensor in ferrous ammonium sulphate has been explained only by recourse to such a wavefunction by Collins et al.<sup>14</sup>.

### 3. QUADRUPOLE SPLITTING

The principal relation giving the hyperfine splitting of nuclear energy due to electric quadrupole interaction is given by

$$E_Q = \frac{e^2qQ}{4I(I-1)} [3I_z^2 - I(I+1) + \eta(I_x^2 - I_y^2)] \quad (15)$$

$$= \frac{e^2qQ}{4I(I-1)} [3I_z^2 - I(I+1) + \frac{\eta}{2} (I_+^2 + I_-^2)]$$

where  $I_{\pm} = I_x \pm I_y$ . Now, eigenvalues  $E_Q^*$  and  $E_Q$  appropriate to the nuclear excited state and the ground state must be calculated.

$$E_Q^* \pm \frac{3}{2} = \frac{e^2qQ}{2} [1 + \eta^2/3]^{1/2} \quad (16)$$

$$E_Q \pm \frac{1}{2} = -\frac{e^2qQ}{2} [1 + \eta^2/3]^{1/2}$$



The resonance energies are now given by the difference between the eigenvalues

$$\Delta E_Q = \frac{e^2 q Q}{2} [1 + \eta^2/3]^{1/2} \quad (17)$$

#### 4. SIGN OF EFG AND REASONS FOR MEASURING IT

Since the electric field gradient is actually a second rank tensor, what really is meant by the sign of  $V_{zz}$  or of  $q$ ? The various theoretical methods employed in calculating the electric field gradients all suffer because of inadequacies of the wavefunctions available for iron ions. Therefore, theoretical estimates of the field gradients are usually not very reliable. However, the sign of EFG is completely determined by the angular part of the wavefunction. The angular part of the wavefunctions is much more reliable than the radial part, and hence, calculations of the sign can be made with some confidence if a realistic method is chosen. Thus the experimental determination of the sign of  $V_{zz}$  is reliable for differentiating between two theoretical models when they lead to different signs.

#### 5. MAGNETIC PERTURBATION

One of the difficulties in studying quadrupole effects in  $\text{Fe}^{57}$  is the presence of only one measurable parameter in powdered, zero magnetic field samples. Ruby and Flinn<sup>15</sup> first suggested an interesting possibility of applying an external magnetic field in order to display more information in the Mössbauer spectrum. It was called magnetic perturbation and its theory was worked out by Collins<sup>16</sup>, and Gabriel and Ruby<sup>17</sup>. Theoretical studies, analytical by Collins<sup>16</sup> and numerical by Gabriel and Ruby<sup>17</sup>, verified that two normally identical lines become markedly different in presence of external magnetic field. By identifying the lines means that the sign of  $V_{zz}$  may be measured in this way. In addition, the fine structure of the perturbed spectra may be examined to yield rough values of asymmetry parameter, within limits deter-

mined by magnetic anisotropy in paramagnetic compounds and by vibrational isotropy of the sample<sup>14</sup>. For the limit of zero asymmetry parameter and for applied magnetic fields of about 25 Koe or more, in the  $Fe^{57}$   $m_I = \pm \frac{3}{2}$  lines appear as triplet and the  $m_I = \pm \frac{1}{2}$  lines appear as doublet. For determining the sign of  $V_{zz}$  of  $Fe^{57}$  doublet occurs at the more positive velocity indicating  $V_{zz}$  positive and vice-versa. As the asymmetry parameter increases, the lines begin to look more alike to the point of becoming identical triplets for an asymmetry parameter of unity, although the exact appearance of the lines depends on whether the magnetic field is parallel or perpendicular to the experimental axis, the direction of the incident radiation.

Collins<sup>16</sup> applied this magnetic perturbation to determine the sign of ferrocene at 4.2K. The sign of  $q$  in some ionic ferrous compounds has also been determined<sup>18</sup>. It must be remarked that this method is applicable to powder samples and most samples are powders rather than single crystals.

## 6. GOLDANSKII-KARYAGIN EFFECT

The intensities for a single crystal absorber are generally not equal. Occasionally in powder sample absorbers also there is asymmetry in the two lines of a  $Fe^{57}$  quadrupole split spectrum. The most obvious reason for intensity asymmetry in powdered samples is simply the preferential orientation. This sort of preferential orientation in powdered samples may be reduced or eliminated by improving sample grinding and or mixing with noninterfering powder such as chalk dust, sugar etc. If still the sample shows the intensity asymmetry it may be due to Goldanskii Karyagin effect.

Karyagin<sup>19</sup> has derived an expression for the ratio of two lines as a function of the difference of the mean - square vibrational amplitudes of the nucleus along and perpendicular to the  $V_{zz}$  axis. Since the recoilless fraction is related to the mean square vibrational amplitude in the direction of the incident gamma, the contribution of each microcrystal in the sample is dependent upon its orientation,

yielding a preferential intensity having an effect similar to preferential orientation. The Goldanski - Karyagin effect may, sometimes, be employed to deduce the sign of  $V_{zz}$ . The reported<sup>20</sup> dependence of intensity ratio upon  $(\langle Z^2 \rangle - \langle X^2 \rangle)$  may be employed to identify the lines and hence the sign of  $V_{zz}$  or conversely sign of vibrational anisotropy can be determined if the sign of  $V_{zz}$  is known. In iron and tin, the  $m_I = \pm \frac{3}{2}$  line is more intense for negative values of the anisotropy parameter  $(\langle Z^2 \rangle - \langle X^2 \rangle)$  and is less intense for positive values.

## 7. IMPORTANCE OF EFG INFORMATION

Generally, the quadrupole splitting has been used in the literature as a sort of measure of distortion of a system from spherical symmetry. Same quadrupole splitting could be shared by two compounds, for example, iron sulphide, (pyrite) and iron sulphide (marcasite); but their strength would differ.

Ingalls<sup>11</sup> has shown that the ligand and valence contributions to  $V_{zz}$  invariably have opposite sign for some systems. Thus at the low temperature limit, where the valence contribution depends neither on distortion nor temperature, increased ligand distortion would decrease  $V_{zz}$  and hence the quadrupole splitting, since the valence contribution would be dominant. At the high temperature limit, the problem would be ligand only and be subject to the difficulties, but would, within those splitting indicates increased distortion. In the intermediate temperature range, where the valence contribution is both temperature and distortion sensitive the story becomes very complicated. The splitting of the  $d$  - orbitals, which determine the valence contribution of distortion, whereas the ligand contribution to the EFG corresponds to  $q/r^3$  type of distortion. Since both contributions increase, in opposite senses in response to two different types of distortion, the meaningful assignment of a distortion - quadrupole splitting relationship for such system at intermediate temperatures require some prior assumptions.

## 8. SINGLE CRYSTAL METHOD FOR EFG DETERMINATION

From the discussion of 'Goldanskii Karyagin effect' it is apparent that peak intensity area ratio may also be a measurable parameter (of iron and tin) of compounds by the use of single crystals. However, to obtain accurate values of EFG parameters it is essential to find a theoretical expression for the area in terms of these parameters.

Following Lang<sup>21</sup>, let us introduce the rate  $fS_0$ , the number of recoilless  $^{144}\text{Kev}$  photons emitted per second into the solid angle subtended by the detector;  $(1-f)S_0$  being the non-recoilless rate. Since the emitted recoilless photons are not actually monoenergetic, but show a distribution of energies centered about  $E_0 \approx 14.4 \text{ Kev}$ , we introduce the function  $S(E-E_0)$ , the number recoilless photons emitted per second per unit energy interval into the same detector angle. If the source is moving with velocity  $V$  relative to absorber, then recoilless photon distribution is actually centered about  $E_0 + (V/C)E_0 = E_0 + \epsilon$  and  $S(E - E_0 + \epsilon) \rightarrow S(E - E_0 - \epsilon)$ .  $S(E - E_0 - \epsilon)$  is a resonance type function with  $\Gamma(\text{FWHM}) = 10^{-7}\%$ , therefore

$$\int_0^{\infty} S(E - E_0 - \epsilon) dE = fS_0 \quad (18)$$

the photon arrival rate  $R(\epsilon)$  at the detector is

$$R(\epsilon) = e^{-\sigma e^m} S(E - E_0 - \epsilon) \exp[f' \sigma(E) \eta] + (1-f') S_0 e^{-e^m} \quad (19)$$

where  $e$  = average surface density of atom

$m$  = surface density of nuclei capable of resonance

$f'$  = recoilless absorption probability

$\sigma(E)$  = energy dependent resonance absorption cross section per nucleus in the presence of EFG when no perturbing fields are present; the resonance when no perturbing fields are present, cross section is given by<sup>22</sup>

$$\sigma(E) = \sigma_0 \Gamma_0^2 / 4 [(E - E_0)^2 + \Gamma_0^2 / 4]^{-1} \quad (20)$$

where

$$\sigma_0 = \frac{2\pi \lambda^2 \cdot (2I' + 1)}{1 + \alpha(2I+1)}$$

$\sigma_0$  = natural linewidth of the excited state

$a$  = internal cross-section coefficient

However, in the solid, the resonance cross-section becomes more complicated due to energy dependent splittings, shifts and broadenings. Since the actual resonance is strictly a nuclear process, the condition

$$\int_0^{\infty} \sigma(E) dE = \sigma_0 \Gamma_0 \frac{\pi}{2} \quad (21)$$

is always fulfilled. Consequently  $\sigma(E)$ , in general, may be written in the form

$$\sigma(E) = \frac{\pi}{2} \sigma_0 \Gamma_0 K(E) \quad (22)$$

where

$$\int_0^{\infty} K(E) dE = 1$$

If the nuclear energy levels are split by H or/and EFG fields so that the various energy transitions can be resolved in a Mossbauer type experiment, then  $K(E)$  may be written in the form,

$$\begin{aligned} K(E) &= \sum_n K_n(E_n, \theta, \phi) \\ &= \sum_n P_n(\theta, \phi) K_n(E - E_n) \end{aligned}$$

where  $K_n(E - E_n)$  = a resonance type function which is chosen to have normalisation

$$\int_0^{\infty} K_n(E - E_n) dE = 1 \quad (23)$$

$P_n(\theta)$  = relative angular dependent absorption probability satisfying the condition

$$P_n(\theta, \phi) = 1 \quad \text{since} \quad \int K(E) dE = 1 \quad (24)$$

The directional dependence of  $P_n$  has its origin in the fact

that H and/or EFG interaction destroys the spherical symmetry of the nuclear environment.

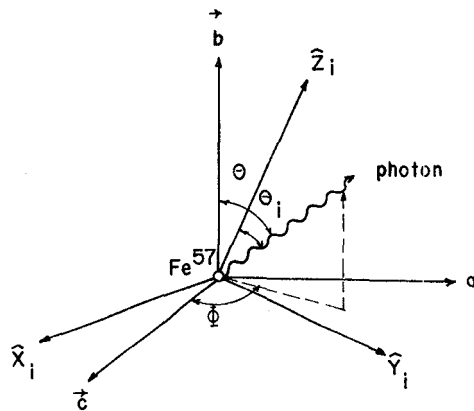
If  $\beta$  is the detector efficiency for 14.4 Kev protons and  $R_B$ , some velocity independent background counting rate, then  $M(\epsilon) = \beta R(\epsilon) + R_B$  the experimental data of interest is actually  $M(\epsilon)/c$  where  $c$  is the count rate independent of source velocity. The area under the  $n^{\text{th}}$  peak  $A_n$  is for  $t_n \ll 1$  and  $(\frac{1}{c}) \int \beta_0 S_0 \exp(-\sigma e^m) = D$  given by

$$A_n = \int_0^\infty f' \omega \sigma_n(E) dE = D \Gamma_0 \left(\frac{\pi}{2}\right) D \Gamma_0 \sigma_0 \omega f'(\theta, \phi) P_n(\theta, \phi) \quad (25)$$

where  $P_n$  = relative absorption probability for transition

$f'$  = recoilless absorption probability.

If X, Y and Z are the principal axes of the EFG at an iron nucleus in the absorber both  $P_n$  and  $f'$  will vary with the orientation angle of the incident photon beam relative to the axes. The angular dependence of  $f'$  results from an anisotropy in the mean square displacement of the vibrating nucleus.



For a single crystal absorber with two or more possible orientations for EFG'S relative to the incident beam, the area ratio is given by

$$\frac{A_n}{A_m} = \frac{\sum_i P_n(\theta_i, \phi_i) f'(\theta_i, \phi_i)}{\sum_m P_m(\theta_i, \phi_i) f'(\theta_i, \phi_i)} \quad (26)$$

In case the absorber is a powder, the expression for the ratio of the area is

$$\frac{A_n}{A_m} = \int_{4\pi} P_n(\theta, \phi) f'(\theta, \phi) d\Omega / \int_0^{4\pi} P_m(\theta, \phi) f'(\theta, \phi) d\Omega \quad (27)$$

The importance of the Debye-Waller factor (or Mössbauer fraction) in determining the intensities of the absorption lines was pointed out by Goldanskii et al. (G.K.E).

Zory<sup>23</sup> and Hien<sup>24</sup> have discussed the analysis of EFG in single crystal absorbers containing Fe<sup>57</sup>, while Karyagin<sup>25,26</sup> has discussed the more general case of a nuclear transition of arbitrary multipolarity, all in the thin absorber limit. Zory<sup>23</sup> applied his analysis to FeCl<sub>2</sub>.4H<sub>2</sub>O and evaluated all the EFG parameters, while Danon and Iannareila<sup>27</sup> used the same analysis to confirm their expectations concerning the field gradient parameters in sodium nitroprusside, Na<sub>2</sub>[Fe(CN)<sub>5</sub>NO].2H<sub>2</sub>O. Ingalls, Ono and Chandler<sup>28</sup> and Chandra and Puri<sup>29</sup> have also applied a similar analysis for the determination of EFG as a function of temperature in Ferrous ammonium sulphate. Chandra and Puri<sup>29</sup> also analysed FeSO<sub>4</sub>.7H<sub>2</sub>O. There are reports, in the literature, of EFG using similar analysis for Fe(KSO<sub>4</sub>)<sub>2</sub>.6H<sub>2</sub>O<sup>30</sup>, FeSO<sub>4</sub>.4H<sub>2</sub>O<sup>31-33</sup>, FeSO<sub>4</sub><sup>34</sup>, FeSiF<sub>6</sub>.6H<sub>2</sub>O (Ref.35-37), FeTiO<sub>3</sub><sup>38</sup>, FeS<sub>2</sub>(p)<sup>39</sup>, FeS<sub>2</sub>(m)<sup>40</sup>, KFeS<sub>2</sub><sup>41-42</sup>, Fe<sub>2</sub>O<sub>3</sub><sup>43,44</sup>, Ferrocene<sup>16</sup>, Siderite<sup>45</sup> etc.

In order to use the above equation let it be expressed in nuclear EFG parameters. Considering the crystal axes  $\vec{a}$ ,  $\vec{b}$ , and  $\vec{c}$  as mutually orthogonal, the unit vectors  $(\hat{X}_i, \hat{Y}_i, \hat{Z}_i)$  locate the principal axes of EFG of  $i^{\text{th}}$  site, the three Euler angles  $(\alpha_i, \beta_i, \gamma_i)$  designating their orientations relative to  $(\vec{a}, \vec{b}, \vec{c})$  being unknown. Angles  $(\theta_i, \phi_i)$  are the orientation angles of the incident beam relative to  $(X_i, Y_i, Z_i)$ . Let us introduce  $(\theta, \phi)$  the polar and azimuthal angles of the incident photon beam relative to  $(\vec{a}, \vec{b}, \vec{c})$  axes.

The expressions for relative transition probabilities  $P_3$  and  $P_1$  were derived utilizing the fact that 14.4 Kev gamma rays is a magnetic dipolar radiation and given by

$$\begin{aligned}
 P_3(\theta, \phi) &= 4(1 + \eta^2/3)^{1/2} + (3 \cos^2\theta_i - 1 + \eta \sin^2\theta_i \cos 2\phi_i) \\
 P_1(\theta, \phi) &= 4(1 + \eta^2/3)^{1/2} - (3 \cos^2\theta_i - 1 + \eta \sin^2\theta_i \cos 2\phi_i)
 \end{aligned}
 \tag{28}$$

Expressing  $\cos^2\theta_i$  and  $\sin^2\theta_i \cos 2\phi_i$  in terms of known experimental angles  $(\theta, \phi)$  and the known Euler angles relating site to axes  $(\vec{a}, \vec{b}, \vec{c})$ , from equations (above) assuming isotropy of  $f'(\theta, \phi)$  one gets

$$\frac{\alpha_3}{\alpha_1} = \frac{\sum_{\text{sites}} \{4(1 + \eta^2)^{1/2} + (3K - 1 + K')\}}{\sum_{\text{sites}} \{4(1 + \eta^2)^{1/2} + (3K - 1 + K')\}}
 \tag{29}$$

where

$$\begin{aligned}
 K &= \sin^2\theta [(\cos^2\phi)Z_a'^2 + (\sin^2\phi)Z_c'^2] + (\cos^2\theta)Z_b'^2 + (\sin^2\theta \sin 2\phi)Z_a'Z_c' \\
 &\quad + \sin 2\theta [(\sin\phi)Z_c'Z_b' + (\cos\phi)Z_a'Z_b'] \\
 K' &= \sin^2\theta [(\cos^2\phi)(X_a'^2 - Y_a'^2) + (\sin^2\phi)(X_c'^2 - Y_c'^2)] + (\cos^2\theta)(X_b'^2 - Y_b'^2) + \\
 &\quad + \sin^2\theta(\sin 2\phi)(X_a'X_c' - Y_a'Y_c') + \sin 2\theta [(\cos\phi)(X_a'X_b' - Y_a'Y_b') \\
 &\quad + (\sin\phi)(X_c'X_b' - Y_c'Y_b')]
 \end{aligned}$$

The symbols  $X_a'$ ,  $X_b'$  etc denote the direction cosines  $\hat{X} \cdot \vec{a}$ ,  $\hat{Y} \cdot \vec{b}$  etc. These direction cosines can be expressed as a function of the same Euler angles  $(\alpha, \beta, \gamma)$ . The schematics of the absorption of 14.4 Kev gamma rays by  $\text{Fe}^{57}$  in single crystals is shown in the figure.

In the above analysis, unfortunately, it has been necessary to use samples of sufficient thickness that the thin absorber analysis can not be completely justified; because the saturation effects can not be neglected. Therefore, it is necessary to have a method of analysis in which saturation is taken into account. Because of polarization dependence of the individual nuclear cross sections the intensities<sup>46</sup> or areas<sup>47</sup> of the absorption lines can not be calculated in the thin absorber approximation. Polarization effects must also be taken into account in making a detailed interpretation of spectra obtained by applying a



magnetic field to a thick, randomly oriented powder of a material exhibiting a quadrupole doublet<sup>15</sup>. Blume and Kistner<sup>48</sup> calculated the intensities transmitted through an absorber of arbitrary thickness in the case where all parameters describing the individual cross sections are known. Housley; Grant and Gonser<sup>49</sup> generalised the Blume and Kistner<sup>48</sup> treatment, for more than one resonant site per unit cell by introducing an average scattering amplitude per unit cell obtained by summing the properly weighted scattering amplitudes from all sites, all scattering amplitude matrices being expressed in terms of same basis polarisations. Housley *et al*<sup>49</sup> obtained formulas relating absorptions as a function to the individual nuclear cross sections for radiation propagating along special directions in the monocrystal which are predictable from crystal symmetry considerations. In these cases the gamma ray beam can be thought of as consisting of two orthogonal intensities each of which propagates through the crystal with its own index of refraction. Housley *et al*<sup>50-52</sup> has shown by means of several examples, the importance of polarisation effect in analysis of data on single crystals or magnetised materials and determination<sup>53</sup> of the sign of the magnetic hyperfine field. Housley, Gonser and Grant<sup>45</sup> determined the Debye Waller factor in Siderite taking into consideration the polarisation terms. Siderite has been of considerable interest and there exist many reports<sup>45</sup>.

## 9. FINITE THICKNESS ANALYSIS

The complex index of refraction for the material is given by<sup>53</sup>

$$n = 1 + \frac{2\pi N}{k^2} F(k, k') \quad (30)$$

where  $k$  and  $k'$  are the wave vectors of the incident the scattered radiation, respectively,  $N$  is the number of resonant nuclei per unit volume, and  $F(k, k')$  is the coherent scattering amplitude for a single nucleus. The quantities  $\bar{F}$  and  $n$  may be replaced by a 2x2 matrix. Generalising, for a complicated crystal having several resonant nuclear sites per unit cell,

$$n = 1 + \frac{2\pi}{k^2} \sum_j N_j F_j(k, k) \equiv 1 + \frac{2\pi}{k^2} F_n(k, k) . \quad (31)$$

Sum runs over all the sites. It is assumed that the electromagnetic interaction is so weak that the index of refraction has a negligible influence on an incident beam in a distance of order of the unit cell dimensions. Now expressing  $n$  in terms of the density matrix rotation.

$$n = 1 + i \frac{\sigma_0}{2k} \sum_{ij} \begin{pmatrix} \rho_{11}^{ij} & \rho_{12}^{ij} \\ \rho_{21}^{ij} & \rho_{22}^{ij} \end{pmatrix} \frac{N_j f_j'}{(x-x_{ij})^2 + 1} - \frac{\sigma}{2k} \sum_{ij} \begin{pmatrix} \rho_{11}^{ij} & \rho_{12}^{ij} \\ \rho_{21}^{ij} & \rho_{22}^{ij} \end{pmatrix} \frac{N_j f_j' (x-x_{ij})}{(x-x_{ij})^2 + 1} \quad (32)$$

here  $j$  and  $i$  represent sites and hyperfine components. The quantity  $x$  is related to the energy  $E$  by  $x = \frac{2E}{\Gamma}$  and  $x_{ij}$ 's correspond to the resonant energies at the different sites. The Debye - Waller factors are no longer assumed isotropic but are the ones appropriate for the direction  $k$ .

In the special case where  $n$  is diagonal, an incident radiation beam may be decomposed into two components with polarisations corresponding to the basis polarisations in which  $n$  is diagonal. Each of these beams may be regarded as separately propagating through the crystal with its own index of refraction.

An effective thickness matrix  $\sigma$  may be defined from the equation (32) and will be diagonal when  $n$  is diagonal

$$\sigma = \begin{pmatrix} \sigma_{11} & \sigma_{12} \\ \sigma_{21} & \sigma_{22} \end{pmatrix} = \sigma_0 \sum_{ij} \begin{pmatrix} \sigma_{11}^{ij} & \sigma_{12}^{ij} \\ \sigma_{21}^{ij} & \sigma_{22}^{ij} \end{pmatrix} \frac{n_j f_j'}{(x-x_{ij})^2 + 1} \quad (33)$$

where  $n_j$  are the number of resonant nuclei of type  $j$  per unit area. When

$n$  is diagonal, the matrix elements of  $\sigma$  can be extracted from experimental line intensities, if the spectra are well resolved.

Assuming that the  $\gamma$  ray beam can be described as a plane wave incident on a slab of homogeneous absorbing material of uniform thickness and that the absorption may be described without dispersion. Describing the polarisation and intensity of the unshifted component of the source radiation at any energy by a density matrix

$$S = \frac{I}{2\pi} \sum_{k, \ell} \begin{pmatrix} \rho_{11}^{k\ell} & \rho_{12}^{k\ell} \\ \rho_{21}^{k\ell} & \rho_{22}^{k\ell} \end{pmatrix} \frac{r_{\ell} f_{\ell}}{(x - x_{k\ell} - v) + i} \quad (34)$$

where  $I$  is the total intensity due to the transition of interest and  $r$  is the fraction of the emitting nuclei in site  $\ell$ . The source resonance energies  $x_{k\ell}$  and site positions  $\ell$  will not generally correspond to those of the absorber. The quantity  $v$  describes the Doppler shift in the resonance energies due to relative motion of the source and absorber. The general expression for the transmitted intensity at a particular energy  $x$  where radiation from a source described by Eq. (34) is incident on an absorber described by equation (33) can easily be found since  $S_{11}$  gives the projection of the transmitted source intensity on one of the basis polarizations and  $S_{22}$  that of the other.

$$I(x, v) = \frac{I}{V} \left[ S_{11} e^{-\sigma_{11}} + S_{22} e^{-\sigma_{22}} \right] \quad (35)$$

This expression is similar to the corresponding expression for unpolarised radiation except for containing two terms instead of one on the right. It may be subtracted from the incident intensity  $S_{11} + S_{22}$  and the result integrated over  $x$  to obtain the fractional absorption dip at a Doppler velocity  $v$ . Integrating over  $v$  to obtain the dimensionless area under the absorption spectrum.

The unknown parameters of the experiment are contained in the  $\sigma$ 's and hopefully can be extracted from measurements made in different directions and/or with different thickness absorbers. If the absorption is

nes are well resolved individual areas can be defined. Assuming source and absorber resonance lines to be of natural width, then after Bykov and Hein<sup>47</sup>, for the overlap of the  $k^{\text{th}}$  source line from site with the  $i^{\text{th}}$  absorber line from site  $j$ , this gives

$$A_{ij}^k = S_{11}(x_{kl})\sigma_{11}(x_{ij}) \exp \left[ \frac{\sigma_{11}(x_{ij})}{2} \right] \left\{ I_0 \left[ \frac{\sigma_{11}(x_{ij})}{2} \right] + I_1 \left[ \frac{\sigma_{11}(x_{ij})}{2} \right] \right\} \\ + S_{22}(x_{kl})\sigma_{22}(x_{ij}) \exp \left[ \frac{\sigma_{22}(x_{ij})}{2} \right] \left\{ I_0 \left[ \frac{\sigma_{22}(x_{ij})}{2} \right] + I_1 \left[ \frac{\sigma_{22}(x_{ij})}{2} \right] \right\} \quad (36)$$

where  $I_0$ , and  $I_1$  are zeroth and first - order Bessel functions of imaginary arguments. When different absorber lines have same energy, their contributions are added in the arguments of functions of equation above.

The dimensionless area  $A_{ij}^{kl}$  is related to the background corrected experimental area  $B$  by

$$A_{ij}^{kl} = 2B/\Pi\Gamma \quad (37)$$

For relatively thin absorbers, power series expansions in equation (36) are useful. If we restrict ourselves for simplicity to a single line unpolarised source  $S_{11} = S_{22} = f/2$  and we define the average cross section on resonance

$$p = |\sigma_{11}(x_{ij}) + \sigma_{22}(x_{ij})|/2 \quad \text{and the fractional polarisation}$$

$$a = \frac{\sigma_{11} - \sigma_{22}}{\sigma_{11} + \sigma_{22}} \quad \text{of the absorption we may write}$$

$$A = p - \frac{1}{4} (i + a^2)p^2 + \frac{1}{16} (1 + 3a^2)p^3 - \frac{5}{384} (1 + 6a^2 + a^4)p^4 + \dots$$

on inverting

$$p = A + \frac{1}{4} (1 + a^2)A^2 + \frac{1}{16} (1 + a^2 + 2a^4)A^3 + \frac{5}{384} (1 + a^4 + 6a^6)A^4 \dots$$

here

$$A = A_{ij}/f \quad (38)$$

Therefore for a relatively thin absorber, the effects of polarisations may be quite small unless fractional polarisations become large.

Equations for the area ratios which have been previously used in analysing the experimental data can be obtained by dropping all but the first term in equation (38).

Grant, Housley and Gonser<sup>12</sup> applied the above corrections to determine the electric field gradient and the mean square displacement tensor parameters at the Fe sites in sodium nitroprusside and found that the principal axes of two tensor do not coincide. Similar analysis was also applied in the case of  $\text{FeSO}_4 \cdot 4\text{H}_2\text{O}$ <sup>33</sup> in the temperature range of 300 -77K.

## 10. USING IPOLARISED RADIATION

The polarisation of  $\gamma$  rays has been reported<sup>54-58</sup> by many workers, and it can take place by the Stark and Zeeman effect that are already familiar in the optical polarisation studies<sup>55</sup>. If the recoilfree  $\gamma$  rays are brought into resonance the matching of polarisation components in the source and the absorber nuclear transitions is required in addition to the usual appropriate Doppler motion. For example, circularly polarised  $\gamma$  rays from a source can only be resonantly absorbed if a transition with the same helicity is offered (conservation of angular momentum). By observing the helicity of circularly polarised  $\gamma$  rays, the sign of magnetic hyperfine field can be determined.

Linearly polarised  $\gamma$  rays<sup>60-62</sup> are of particular interest. Some methods for producing 14.4 Kev linearly polarised  $\gamma$  rays are briefly described below;

One simple method is to use a magnetically source matrix (iron foil) and to magnetise it in a fixed direction. With iron foil it is

convenient to magnetise perpendicular to the direction of emission. The emitted radiation is then not monochromatic but consists of six individual components with intensity ratios 3:4:1:1:4:3 each of which has a definite polarisation. In the case we are considering  $\pm 3/2 \rightarrow \pm 1/2$  and  $\pm 1/2 \rightarrow \pm 1/2$  transitions have a linear polarisation with the electric vector vibration parallel with respect to the magnetisation, and  $\pm 1/2 \rightarrow \pm 1/2$  transitions are similar but perpendicularly polarised. In a single crystal absorber, if the source and absorber are directionally polarised by a magnetic field which can be internal in origin or by an electric field such as is associated with the electric field gradient tensor, the polarisation of each emission line becomes important. The relative orientation of the principal directions in the source and the absorber will cause variation of the line intensity. Detailed theory of the line intensities has been reported<sup>63,64</sup>. One of the first applications of an iron foil source was in the determination of the sign of the quadrupole coupling constant in a single crystal of  $\text{FeSiF}_6 \cdot 6\text{H}_2\text{O}$ <sup>65</sup>.

The assignment of hyperfine components in a complex spectrum would be easier if the source was effectively polarised and monochromatic so that the resonant absorption would only be observed in those transitions with the same polarisation. This method was first demonstrated by Housley<sup>66</sup> using a paramagnetic single crystalline source exhibiting a quadrupole split spectrum. If the  $V_{zz}$  principal axis of the EFG is perpendicular to the direction of observation the  $\gamma$  rays corresponding to the  $\pm 3/2$  transition are totally linearly polarised and the  $\gamma$  rays corresponding to  $\pm 1/2$  transition are partially linearly polarised. This more intense line can be selectively filtered out. The asymmetry parameter should be zero to ensure that the nuclear wavefunctions are pure  $|m\rangle$  states.

An equivalent method which does not require a split source is to use a polariser. This was first demonstrated using iron foils magnetised perpendicular to the propagation<sup>67</sup> and more recently using a polycrystalline sample of Yttrium iron garnet (YIG).

When source and absorber exhibit a hyperfine interaction, the polarisation of the  $\gamma$  rays has to be taken into account in deriving the relative line intensities<sup>56,69</sup>. By analysing the line intensities ob-

tained from a source emitting linearly polarised recoilfree  $\gamma$  rays and a single crystal absorber cut in an arbitrary direction, one can determine the spin orientation and the principal axes of the EFG with respect to the crystal axes<sup>6,16,17,65,70,71</sup>. Daniels<sup>72</sup> has considered the problem of calculating line intensities in Mössbauer absorption using the polarised gamma rays polarised absorbers with especial reference to Fe<sup>57</sup>.

The polarisation dependence has been reported in a number of theoretical studies<sup>49,57,63,73-79</sup> and various techniques have been used to carry out polarimetry experiments based on transversely magnetised CO<sup>57</sup>( $\alpha$ Fe) source<sup>51,52,58,60,61,64,68,71,74,80-88</sup> or by filter technique<sup>56,60,62,64,89</sup>. Multiplicity resulting from the six linearly polarised lines or inefficiency of the selective excitation or of the filters in terms of intensity, degree of polarisation and non Lorentzian lines are some of the disadvantages of the above methods. Sources exhibiting quadrupole hyperfine interaction will circumvent some of the problems. The utility of a quadrupole split CO<sup>57</sup> source for a polarimeter depends on fulfillment of following conditions.

The material can be grown as a single crystal and cutting of thin plates in various directions is possible.

CO<sup>57</sup> can be incorporated with a unique charge state and a crystallographically unique resonance site.

The lattice site should have axial symmetry with unique orientations.

The quadrupole splitting should be large or at least well resolved.

Gonser, Sakai and Keune<sup>90</sup> reported a quadrupole Fe<sup>57</sup> polarimeter consisting of single crystal of LiNbO<sub>3</sub>:CO<sup>57</sup> as source (polariser) and FeCO<sub>3</sub> (siderite) as a absorber (analyser). The possibility of using two identical single crystals as polariser and analyser has been mentioned by Goldanskii *et al.*<sup>45</sup> and Gibb<sup>86</sup> used it as a means of determining the directional data normal to the observation axis in the case of ferrous ammonium sulphate and the EFG was determined by using crystals grown on one particular face ( $\bar{2}01$ ) so that the observation direction was nor-

mal to the b axis and at  $47.3^0$  to the c axis in the ac plane. This type of measurements have difficulty in measuring an accurate thickness curve and because of the large time involved. The choice of the parameters to fit the data is also not unambiguous. Gibb<sup>87</sup> made further experiments on ferrous ammonium sulphate using a  $Co^{57}/Fe$  foil source magnetised in the plane of the foil and perpendicular of observation by mounting the source in between the poles of a permanent magnet. Thus, most inner and outer pair of lines were plane polarised while parallel to the applied magnetic field, and the other two lines are polarised perpendicular to the field.

Because of the self absorption in the source matrix, and, also due to incomplete polarisation of the foil in absence of the applied magnetic field is not strong enough, the predicted intensity ratios (3:4:1:1:4:3) are unlikely to be achieved. Gibb<sup>91,92</sup> redetermined the electric field gradient tensor in  $FeCl_2 \cdot 4H_2O$  using a polarised Mössbauer source in the same method. Spiering and Vogel<sup>93</sup> calculated the absorption cross section for a polarised single crystal absorber of finite thickness using a intensity matrix method and applied it in the case of  $FeCl_2 \cdot 4H_2O$ . Zimmermann<sup>94</sup> also made experiment on  $FeCl_2 \cdot 4H_2O$  using the intensity tensor method.

## REFERENCES

1. M.H.Cohen and R.Reif in *Solid State Physics*, ed. F.Seitz and D.Turnbull (Academic Press, New York 1957).
2. S.P.Puri, *Procd. Nuclear Physics and Solid State Physics Symposium* December 28-31, 1969, Roorkee, India, 1, 71 (1969).
3. J.C.Travis in *An Introduction to Mössbauer Spectroscopy*, ed, Leopold May (Plenum Press, New York, 1971).
4. B.D. Dunlap in *Mössbauer Effect Data Index (1970)* ed. John G.Stevens and Virginia E. Stevens (Plenum Press, New York 1971). p. 25.
5. R.M.Sternheimer, *Phys. Rev.* 80, 102 (1950).
6. Ref. 1 page 324.
7. A.J.Freeman and R.E.Watson, *Phys. Rev.* 131, 2566 (1963).
8. R.Ingalls, *Phys. Rev.* 128, 1155 (1962).



9. R.M.Sternheimer, Phys. Rev. 130, 1433 (1963) .
10. F.A.Cottan and G.Wilkinson in *Advanced Inorganic Chemistry*, (Int. publishers, New York 1963) p.563.
11. R.Ingalls, Phys. Rev. 133, A787 (1964) .
12. R.W.Grant, R.M.Housley and U.Gonser, Phys.Rev.178, 523 (1969).
13. E.Fluck, W.Kerler and W.Neuwirth, Agnew Chem. 20, 277 (1963).(International edition) .
14. R.L.Collins and J.C.Travis in *Mössbauer Effect Methodology*, Vol.3,ed. I.J.Gruverman (Plenum Press, New York 1967) .
15. S.L.Ruby and P.A.Flinn, Rev.Mod.Phys. 36, 351 (1964) .
16. R.L.Collins, J.Chem. Phys. 42, 1072 (1965).
17. J.R.Gabriel and S.L.Ruby, Nucl. Instru. Methods 36, 23 (1965).
18. R.W.Grant, H.Widersich, A.H.Muir, Jr., U.Gonser and W.N.Delgass, J. Chem. Phys. 45, 1015 (1966) .
19. S.V.Karyagin, Proc. Acad. Sci. USSR, Phys. Chem. Sec. 148, 110 (1964). (English Translation) .
20. P.A.Flinn, S.L.Ruby and W.L.Kehl, Scientific paper 63-128.117, p.6, Westinghouse Research Laboratories, Beulah Road, Churchill Borough, Pittsburgh, Pennsylvania, U.S.A.
21. G.Lang, Nucl. Instru. Methods 24, 425 (1963).
22. J.D.Jackson, Can. J. Phys. 33, 595 (1955).
23. P.Zory, Phys. Rev. 140, A1401 (1965).
24. P.Z.Hien, Soviet Phys. JETP 22, 1080 (1966) .
25. S.V.Karyagin, Soviet Phys. Solid State 8, 1387 (1966) .
26. S.V.Karyagin, Soviet Phys.Solid State 9, 1979 (1968) .
27. J.Danon and L.Iannarella, J.Chem.Phys. 47, 382 (1967) . Ref. 12 also. M. H. Clear, J.F.Duncan and D.McConchie, J.Royal Soc.New Zealand 1, 71 (1971) .
28. R.Ingalls, K.Ono and L.Chandler, Phys. Rev.172, 295 (1968).
29. K.Chandra and S.P.Puri, Phys. Rev. 269, 272 (1968).
30. V.K.Garg and S.P.Puri, J. Inorg.Nucl.Chem. 35, 2795 (1973) .
31. V.K.Garg and S.P.Puri, J.Chem.Phys. 54, 209 (1971).
32. V.K.Garg and Y.S.Liu, J.Chem.Phys. 62, 56 (1975) .
33. M.S. Nascimento and V.K.Garg, J.Chem.Phys., 66, 5798 (1977) .
34. H.N.Ok, Phys. Rev. B, 4, 3870 (1971) .
35. C.E.Johnson in *Hyperfine Structure and Nuclear Radiations* ed.E. Mat-

- thias and D.A. Shirley (North Holland publishing co., Amsterdam, 1968) p.226.
36. V.K.Garg and K.Chandra, Phys.Stat.Solidi (b) 50, K49 (1972).
  37. J.Chappert, G.Jenhanno, F.Varret, in *Procd. Int. Conf. Mössbauer Spectroscopy*, Cracow, Poland 30 August 1975 Vol. 1, 2C-9, p.161.
  38. V.K.Garg and S.P.Puri, Phys.Stat. Solidi (b) 44, K44 (1971).
  39. V.K.Garg, Y.S.Liu and S.P.Puri, J.Appl.Phys. 45, 70 (1974) and reference therein. P.A.Montano and M.S.Seehra, Solidi State Comm. 20, 879 (1976).
  40. R.Garg and V.K.Garg, Appl.Phys. 16, 75 (1978).
  41. R.Garg, A.C.Oliveira and V.K.Garg, Phys. Stat. Solidi (b) 84, K17 (1977).
  42. R.B.Scorzelli, C.A.Taft, J.Danon and V.K.Garg, J.Phys. C. Solid State Physics 11, 1379 (1978).
  43. T.Ruskov, T.Tomov and S.Georgiev, Phys. Stat. Solidi (a) 37, 295 (1976) and reference therein.
  44. A.N.Salugin, V.A.Povitskii, M.V.Filin, V.M.Erkin and V.V. Dudoladov, Soviet Phys. Solid State 16, 792 (1974).
  45. R.M.Housley, U.Gonser and R.W.Grant, Phys.Rev.Letts. , 1279 (1968). D. L. Nagy, I.Dezsi and U.Gonser, Neues.Jahrb.Mineral.Monatsh 3, 101 (1975). I.P.Vinogradov, A.M.Pritchard, E.F.Makarov and I.P.Suzdalev, Solid State Comm. 8, 965 (1970). V.I.Goldanskii, E.F.Makarov, I.P. Suzdalsv and I.P.Vinogradov, Phys. Rev. Letts. 20, 137 (1968) JETP 27, 44 (1968).
  46. J.G.Dash, R.D.Taylor, D.E.Nagle, P.P.Craig and W.M.Visscher, Phys. Rev. 122, 1116 (1961).
  47. G.A.Bykov and Pham Zey Hien, Zh. Eksperim. i Teor. Fiz. 43, 909(1962). Soviet Physics JETP 16, 646 (1963).
  48. M.Blume and O.C.Kistner, Phys. Rev. 171, 417 (1968).
  49. R.M.Housley, R.W.Grant and U.Gonser, Phys.Rev. 178, 514 (1969).
  50. R.M.Housley in *Mössbauer Effect Methodology*, Vol.5, ed. I. J. Gruvernan, Plenum Press, New York (1970).
  51. R.M.Housley and U.Gonser, Phys.Rev.171, 480 (1968).
  52. U.Gonser and R.M.Housley, Phys.Rev. Letts. 266, 157 (1968).
  53. M.Lax, Rev. Mod. Phys. 23, 287 (1951).
  54. G.J.Perlow, S.S.Hanna, M.Hamermesh, C.Littlejohn, D.H.Vicent, R.S. Preston and S.Heberle, Phys. Rev. Letts. 4, 74 (1960).

55. W.A.Shurcliff - *Polarised Light production and Use* (Oxford University Press, London, 1962).
56. S.S.Hanna, J.Heberle, C.Littlejohn, G.J.Perlow, R.S.Preston, and D. H.Vicent, Phys. Rev. Letts, 4, 177 (1960).
57. H.Wegener and F.E.Öbenschain, Z.Physik 163, 17 (1961).
58. A.Kastler, Compt. Rend. 255, 3397 (1962).
59. N.Blume and L.Grodzins, Phys. Rev. 136, A133 (1964).
60. P.Imbert, J.Physique 27, 429 (1966).
61. U.Gonser, p.343 in *Hyperfine Structure and Nuclear Radiations* ed. E. Matthias and D.A. Shirley, North Holland Publishing Co., Amsterdam, (1968).
62. J.P.Stampel, P.A. Flinn in *Mössbauer Effect Methodology* Vol.6, ed. I.J.Gruverman, Plenum Press, New York, (1971).
63. H.Fraunfelder, D.E.Nagle, R.S.Taylor, D.R.F.Cochran and W.M.Visschar, Phys.Rev. 126, 1065 (1962).
64. J.T.Dehn, J.G.Marzolf and J.F.Salmon, Phys. Rev. 135, B 1307 (1964).
65. C.E.Johnson, W.Marshall and G.J.Perlow, Phys.Rev. 126, 1503 (1962).
66. R.M.Housley, Nucl. Instr. Methods, 62, 321 (1968).
67. S.Shtrikman, Solid State Commun. 5, 701 (1967).
68. S.Shtrikman and S. Somekn, Rev. Sci. Instru. 40, 1151 (1969).
69. U.Gonser in *Hyperfine Interactions* ed. A.J.Freeman and R.B. Frankel, (Academic Press, New York, 1967).
70. U.Gonser, R.W.Grant, H.Wiedersich and S.Geller, Appl. Phys. Letts. 9, 18 (1966).
71. U.Gonser and R.W.Grant, Phys. Stat. Solidi 21, 331 (1967).
72. J.M.Daniels, Nucl. Instru.Methods 128, 483 (1975).
73. Y.M.Aizazyán, V.A.Belyakov, Sov.Phys.Solid State 13, 808 (1971).
74. A.V.Mitin, Phys. Stat. Solidi (b) 53, 93 (1972).
75. J.P.Hannon, N.J.Carron, G.T.Trammell, Phys.Rev. B, 9, 2791 (1974).
76. J.P.Hannon, N.J.Carron, G.T.Trammell, Phys.Rev. B, 9, 2810 (1974).
77. D.Barb, M.Rogalski, J.Chim. Phys. Phys.Chim.Biol. 72, 470 (1975).
78. D.Barb, *Proc.Intern. Conf. Mössbauer Spectroscopy*, Cracow, Poland (1975) p. 379, Vol. 2.
79. R.W. Grent in *Mössbauer Spectroscopy - Topics in Applied Physics*, Vol. 5, ed. U.Gonser (Springer Verlag, Berlin, 1975).
80. C.E.Johnson, J.Phys. C. 2, 1996 (1969).
81. R.W.Grant and S.Geller, Solid State Commun. 7, 129 (1969).
82. S.Gellei-, R.W.Grant, L.D.Fullmer, J.Phys.Chem.Solids 31, 793 (1970).

83. R.W.Grant, J.Appl.Phys. 42, 1619 (1971).
84. H.D.Pfanner, U.Gonser, Nucl.Instru.Methods 114, 297 (1974).
85. S.Morup, J. Physique, Colloq. C6, 683 (1974).
86. T.C.Gibb, J.Phys. C.Solid State Phys. 7, 1001 (1974).
87. T.C.Gibb, J.Phys. C.Solid State Phys. 8, 229 (1975).
88. H.Fischer, U.Gonser, H.D.Pfannes and T.Shinjo, *Proc. Intern. Conf. Mössbauer Spectroscopy*, Cracow, Poland p. 463 (1975) Vol.1.
89. F.Varret, P.Imbert, G.Jehanno and R.Saint-James, Phys.Stat. Solidi (a) 27, K99 (1975).
90. U.Gonser, H.Sakai and W.Keune, J.Physique C6, 709 (1976).
91. T.C.Gibb, Chem.Phys. 7, 449 (1975).
92. T.C.Gibb, J.Chem.Soc.Dalton Trans. 743 (1968).
93. H.Spiering and H.Vogel, Hyperfine Interac. 3, 221 (1977).
94. R.Zimmermann, Chem. Phys. Letts, 34, 416 (1975).